Conference Proceedings

Solar World Congress 2015
Daegu, Korea, 08 – 12 November 2015

Numerical model for pressure drop and flow distribution in a solar collector with horizontal U-connected pipes

Federico Bava[1] and Simon Furbo[1]

[1] DTU Civil Engineering, Technical University of Denmark, Brovej, Building 118, 2800 Kgs. Lyngby (Denmark)

Abstract

The development of a numerical model for calculating the pressure drop and flow distribution across a solar collector in isothermal conditions is described in this paper. More specifically, the considered collector layout is that of a harp collector with U-type configuration. The different hydraulic resistances causes unbalance of flow distribution in the absorber pipes, so this aspect had to be considered in order to correctly evaluate the pressure drop. The model was written in Matlab and makes use of pressure drop correlations found in literature for both friction losses and local losses. The model was compared in terms of overall pressure drop against measurements which were performed on an Arcon Sunmark HT 35/10 collector. Different flow rates, temperatures and fluid types were tested during this validation process. In case of pressure drops larger than 1 kPa, the relative error between model and measurements was no larger than 7%, while the absolute average value no larger than 3%. For smaller pressure drops the relative difference was usually larger, but still within the accuracy of the differential pressure sensor. Concerning the flow distribution, it was found that the flow regime was the main parameter affecting the results. Turbulent regime resulted in a much more uniform flow distribution across the absorber pipes compared to laminar regime.

Keywords: *solar collector, pressure drop, flow distribution, friction losses, propylene glycol, heat transfer fluid, temperature, flow rate.*

1. Introduction

The pressure drop over a solar collector is a parameter which must be known and taken into account, when connecting collectors in a solar collector field both in series and parallel. In fact, the pressure drop influences the flow distribution throughout the field, affecting its overall efficiency and energy output, and determines the requirements of the pumps which need to be installed to supply the field in the most efficient way.

The standard norm ISO 9806 does not provide strict guidelines on how to measure the pressure drop characteristic curve, as it states that "the fluid used in the collector for the test shall be water or a mixture water/glycol (60/40), or a mixture recommended by the manufacturer. The temperature of the fluid shall be (20±2) °C" (ISO 9806). Additionally, the conditions during the test may differ significantly from the actual operating conditions of the collector, both in terms of fluid type and temperature. For this reason, it could be useful to have a model able to derive the pressure drop of a collector for different temperatures and fluids, starting from a single test carried out in a specific operating condition.

The most common layout used when manufacturing large flat plate collectors is harp U-type layout, where a number of parallel pipes connecting two manifolds, which have inlet and outlet on the same side. Almost all solar collector field. On the other hand, the parallel pipe design has the disadvantage that perfectly uniform flow distribution cannot be achieved. The flow distribution in flat plate collectors with parallel pipes has been the topic of many investigations, as it may strongly affect the collector efficiency. In fact, several studies show that the efficiency diminishes for decreased uniformity of flow distribution, as a consequence of non-uniform outlet temperatures for the different collector pipes (Chiou, 1982). Wang and Wu (1990) proposed a discrete numerical model to predict the flow distribution in solar collector arrays with vertical

doi:10.18086/swc.2015.10.01 Available at http://proceedings.ises.org

pipes in U-type configuration, taking into account buoyancy force. The flow rate in the riser tubes decreases monotonically with the inlet manifold distance. The same trend was found by Jones and Lior (1994), who considered a single collector with vertical pipes and neglected buoyancy. Weitbrecht et al. (2002) carried out both an experimental and analytical study on the flow distribution in a Z-type collector, investigating the influence that the inset of a pipe into the manifold has on the pressure drop across the tee junction. However, only laminar flow and one specific tee geometry are considered.

Fan et al. (2007) studied the flow and temperature distribution in a large solar collector with 16 U-connected horizontal tubes. A numerical model, based on CFD calculations and taking into account buoyancy, and experimental measurements are compared. The results show that the flow distribution is dominated by friction (and hence buoyancy can be neglected), if the velocity in the collector pipes is high compared to the temperature rise across the collector. In large solar collector fields in Denmark each row usually consists of a number of collectors between 10 and 25 (Windeleff and Nielsen, 2014), so the temperature rise in each collector is relatively small, while the flow rate is relatively high. Consequently, it can be considered that buoyancy plays a minor role in the flow distribution in this kind of installations.

The aim of the study presented in this paper was to develop a numerical model for calculating the pressure drop over a U-type collector. Benchmark of the model was a solar collector for large collector fields, so the flow across the collector could be considered controlled by friction only and the model was developed accordingly.

2. Material and method

2.1. Solar collector design

The developed model was based on the design of U-type large scale collectors. These collectors usually have a number of horizontal pipes welded to absorber strips and connecting two vertical manifolds located along the sides of the collector with their outlet at the top corners of the external frame (Figure 1).

Figure 1: Sketch of a U-type absorber with horizontal pipes.

The choice of this design for the model was motivated by the fact that this is the most frequently adopted design when manufacturing large collectors for solar heating field applications. In fact, these collectors are easy to assemble and quick to connect to one another when they are installed side by side in a field.

The developed numerical model was validated in terms of pressure drop against measurements carried out on a collector of this type, more specifically an Arcon Sunmark HT-SA 35/10 collector, having an aperture area of 12.60 m^2. The collector piping was made of copper and had circular cross section. The 18 horizontal pipes were 5.80 m long, had an inner diameter of 9.1 mm and an intermediate spacing of 122 mm. The manifolds had an inner diameter of 32.9 mm.

Though, as long as the general collector design is preserved, the model can be easily modified to treat also collectors having for example a different number of horizontal pipes, various manifold and pipe diameters.

2.2. Pressure drop correlations

In a solar collector, as well as any other hydraulic circuit, the total pressure drop is given by the sum of two types of pressure losses: friction (or major) losses and local (or minor) losses. Friction losses occur in pipe flow because of viscous effects generated by the pipe surface. Local losses are due to variations of the velocity vector. Valves, bends, tees and abrupt changes in a pipe cross-sectional area are examples of components causing local pressure losses.

The friction loss along a straight pipe of constant cross section is a function of the flow velocity, pipe length, pipe diameter and a friction factor which strongly depends on whether the fluid flow is turbulent or laminar. This pressure loss is calculated by the Darcy-Weisbach equation:

$$\Delta p = \lambda \frac{l}{D_h} \frac{\rho w^2}{2} \qquad \text{(eq.1)}$$

where Δp is the pressure drop [Pa],

λ is the Darcy friction factor [-],

l is the pipe length [m],

D_h is the pipe hydraulic diameter, which equals the inner diameter for a full flow circular pipe [m],

ρ is the fluid density [kg m^{-3}],

w is the mean fluid velocity [m s^{-1}].

As mentioned above, the friction factor depends on the type of flow regime and, if this is turbulent, on the roughness of the pipe as well. The parameter indicating whether a flow is laminar or turbulent is the Reynolds number, defined as

$$Re = \frac{w \rho D_h}{\mu} \qquad \text{(eq.2)}$$

where Re is the Reynolds number [-],

μ is the fluid dynamic viscosity [Pa s].

Density and viscosity are properties characteristic of each fluid and are strongly dependent on the temperature. Water and propylene glycol/water mixtures are the most common fluids used in solar thermal applications. Water thermophysical properties are well known and are easily found in literature. For the density, (eq.3) was used, while the dynamic viscosity was evaluated through (eq.4).

$$\rho = 1000.6 - 0.0128\ T^{1.76} \qquad \text{(eq.3) (Furbo, 2015)}$$

$$\log_{10} \mu = \log_{10} (1.002 \cdot 10^{-3}) + (20 - T)/(T + 96) \cdot [1.2378 - 1.303 \cdot 10^{-3}\ (20 - T) + 3.06 \cdot 10^{-6}\ (20 - T)^2 + 2.55 \cdot 10^{-8}\ (20 - T)^3] \qquad \text{(eq.4) (Kestin, 1978)}$$

Given the large variability of the properties of propylene glycol/water mixtures found in literature and in product datasheets, these were experimentally investigated at the Department of Chemical Engineering of the Technical University of Denmark, making use of an Anton Paar DMA 4100 densimeter and an Anton Paar AMV 200 viscometer. Three samples with glycol concentration of 40%, 45% and 50% were tested at temperatures between 20 °C to 80 °C with an intermediate step of 10 °C. The experimental data points were then interpolated with the polynomial expressions (eq.5) and (eq.6).

$$\rho = 1013 - 0.2682\ T + 0.7225\ x - 1.94 \cdot 10^{-3}\ T^2 - 4.964 \cdot 10^{-3}\ x\ T \qquad \text{(eq.5)}$$

$$\mu = (-2.881 - 6.721 \cdot 10^{-3}\ T + 0.2839\ x + 1.959 \cdot 10^{-3}\ T^2 + -7.036 \cdot 10^{-3}\ x\ T - 1.883 \cdot 10^{-5}\ T^3 + 4.862 \cdot 10^{-5}\ x\ T^2) \cdot 10^{-3} \qquad \text{(eq.6)}$$

where T is the fluid temperature [°C],

x is the mass concentration of propylene glycol in the mixture [%].

Laminar flow regime is characterized by low values of Reynolds number, while turbulent flow occurs for higher values. In literature it is often stated that, for fully developed flow in a circular pipe, laminar flow occurs for Re<2300, and turbulent flow for Re>4000 (Holman, 2002). The flow regime between laminar and turbulent is referred to as transitional regime. In reality, the exact value at which change in flow regime occurs is extremely difficult to determine and depends on whether small disturbances are present. In the developed model, flow was assumed laminar for Re<2300, and turbulent for Re>3100, as a result of a series of tests carried out to evaluate transition in flow regime in the HT collector pipes.

In case of laminar flow, Darcy friction factor was calculated through Hagen-Poiseuille law:

$$\lambda = \frac{64}{Re} \qquad \text{(eq.7)}$$

For turbulent flow in smooth pipes, Blasius correlation (eq.8) was used, as the collector manifolds and pipes were made of commercial copper tubes, characterized by very small absolute roughness (Binder, 1973).

$$\lambda = \frac{0.3164}{Re^{0.25}} \qquad \text{(eq.8)}$$

Although not used in the present study, other friction factor correlations were implemented in the model, such as those proposed by Colebrook (1939) and Haaland (1983) for turbulent flow in pipes of known roughness, and by Joseph and Yang (2010) for any flow regime in smooth pipes.

Following the example of Jones and Lior (1994), the friction factor in the transition region (2300<Re<3100) was calculated by linear interpolation between the value obtained from (eq.7) for Re=2300 and that obtained from (eq.8) for Re=3100.

Regarding local losses, in the solar collector under investigation the only discontinuities were represented by the tees connecting the horizontal pipes to the manifolds. The correlations used to model the pressure losses in tees were mainly obtained by Idelchik (1994). Though, Idelchik's correlations refer to tees with sharp edges and without any inset, while the collectors under investigation presented 2-3 mm inset of the horizontal pipes into the manifold. As even short insets have been proven to be able to affect the pressure drop across tees (Ohnewein et al., 2015), Idelchik's correlations were corrected based on the results from Ohnewein et al. (2015).

2.3. Numerical model

Using the pressure drop correlations described in the previous section, a numerical model was developed in Matlab in order to compute the flow distribution and the resulting pressure drop across the collector. The input data to the model are design characteristics of the collector hydraulics and operating conditions of the heat transfer fluid (type of fluid, volume flow rate and temperature). The fluid temperature, which is assumed to be constant throughout the collector, is used to determine density and viscosity of the fluid.

Given an initial flow rate as input, the model assumes that this flow is uniformly distributed in all horizontal pipes and the resulting pressure drop for each of the possible fluid paths is calculated. Because a uniformly distributed flow is assumed, the pressure drop increases from one strip to the next (see strip numbering in Figure 1), as the fluid path becomes longer due to additional manifold segments. In reality, the pressure drop has to be the same, irrespective of the path the fluid follows, resulting in an adjustment of the flow rate in each strip.

2.4. Experimental setup for pressure drop measurements

To validate the model, the pressure drop across a large solar collector was measured in different operating conditions and compared to the value given by the model. The collector used for this purpose was a HT-SA 35/10 manufactured by the Danish company Arcon-Sunmark (see Section 2.1).

A differential pressure sensor TA-SCOPE from the company TA Hydronics, was used to measure the pressure drop across the collector. The instrument has a nominal accuracy which is given by the higher value between 0.1 kPa and 1% of the measured value.

The flow rate supplied to the collector was measured by a Kamstrup MP115 electromagnetic flow meter. Its accuracy is stated to be within ±0.5%. Additionally, the instrument was tested with different fluids,

temperatures and flow rates at the end of the pressure drop tests and its nameplate calibration factor was confirmed.

Transparent plastic pipes were connected to the inlet and outlet of the collector at one end and to the pressure sensor at the other end, as shown in

Figure 2. The transparent pipes made it easier to verify that no air was present in the circuit, which otherwise would alter both flow rate and differential pressure measurements.

Figure 2: Solar collector HT-SA 35/10 used for the validation and plastic pipes arrangement for pressure drop measurement.

Pressure drop measurements were carried out for different flow rates (between 0.08 and 0.72 liters s-1, corresponding to 0.3 and 2.6 m3 h-1) and at two temperature levels (approximately 25 °C and 70 °C), both using pure water and a 50% propylene glycol/water mixture as heat transfer fluid. The tests were performed in cloudy sky conditions, so that the temperature rise across the collector was negligible and the assumption of isothermal flow introduced in the model was fulfilled.

3. Results

3.*1. Validation of the model*

The comparison between measured and calculated pressure drops as function of the flow rate is shown in Figure 3 and Figure 4 for water and 50% propylene glycol/water mixture. Given the configuration of the hydraulic circuit, it was possible to test volume flow rates up to 2.6 m^3 h^{-1}, corresponding to pressure drops

of approximately 9-10 kPa. The lower boundary of the tested flow rate was determined by the error of the differential pressure sensor, which became increasingly predominant when measuring pressure drops lower than 1 kPa.

Note that the data points referred to as "25 °C" were actually characterized by mean fluid temperatures between 19 °C and 33 °C while those at "70 °C" between 67 °C and 77 °C.

In both diagrams, the typical quadratic relation between pressure drop and flow rate can be observed, as the different groups of points are approximately aligned along parabolic trajectories. Additionally, the influence of the fluid temperature on the pressure drop across the collector can be noted by comparing the different series of points within the same diagram. As expected, a fluid flow at lower temperature caused a higher pressure drop, provided that equal flow rates are compared.

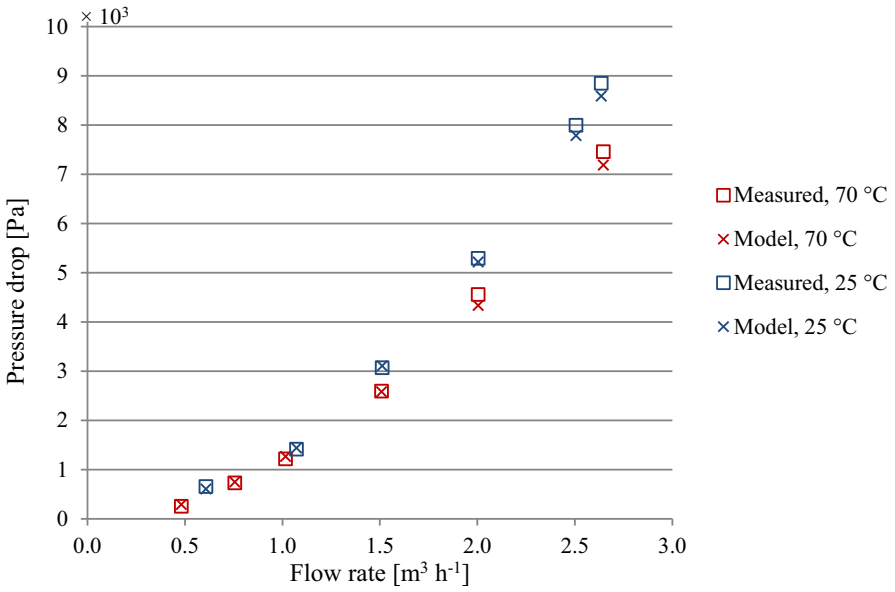

Figure 3: Comparison between measured and calculated pressure drops for water.

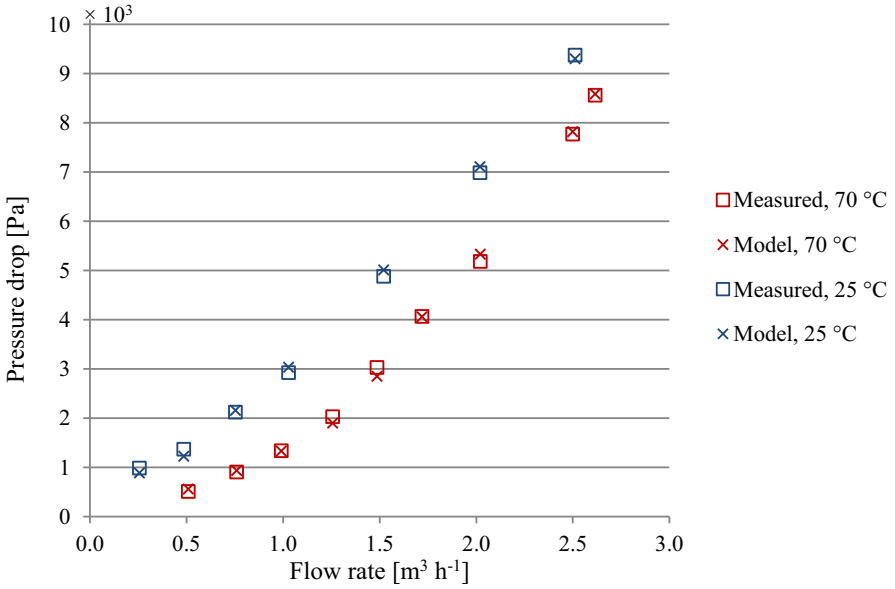

Figure 4: Comparison between measured and calculated pressure drops for 50% propylene glycol/water mixture.

3.2. Flow distribution

Using the developed model, it was possible to calculate the flow distribution inside the HT 35/10 collector at different flow rates and fluid types. The case with water at 20 °C was investigated. Water flow across the horizontal pipes of the collector was either laminar or turbulent at a temperature of 20 °C depending on the flow rate.

The flow distribution is shown Figure 5, where the flow distribution is expressed in terms of the parameter χ, defined by (eq.9) as:

$$\chi_i = \frac{V_i}{\sum_{i=1}^{18} V_i} \qquad \text{(eq.9)}$$

where χ_i is the fraction of the total collector flow rate flowing in the i-th horizontal pipe [-],

V_i is the volume flow rate in the i-th horizontal pipe [m^3 h^{-1}].

In case of a perfectly uniform flow distribution, the parameter χ would have a constant value of 5.56%, regardless of the horizontal pipe number.

The flow distributions shown in Figure 5 are decreasing, from the top to the bottom of the collector, with the only difference being the slope of the profiles.

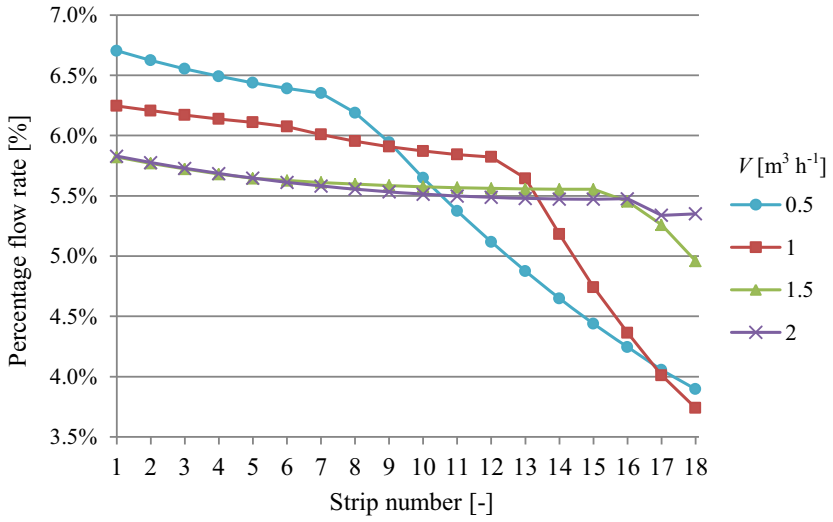

Figure 5: Flow distribution inside the collector at different flow rates for water at 20 °C.

As can be seen in Figure 5, in case of flow rates of 0.5 and 1 m^3 h^{-1}, laminar regime took place and a much less uniform distribution occurred. In these conditions χ varied between 3.7% and 6.7%. For higher flow rates the flow regime became turbulent and the flow distribution became more uniform and similar to that of water at 70 °C.

Although the pressure drop across the horizontal pipes played the most significant role in all cases, its importance for the different paths was quite different, depending on the flow regime. In case of turbulent regime in all horizontal pipes, the pressure drop along these represented 85%-89% of the total collector pressure drop for the top pipe, and 75%-77% for the bottom pipe. The remaining part was caused by forward and return manifolds as well as tee junctions. In case of laminar regime, the pressure drop in the horizontal pipe was 86%-92% of the total for the top pipe, and 48%-54% for the bottom pipe.

4. Discussion

The pressure drop values given by the model matched the measured values with a reasonable accuracy. If pressure drops higher than 1 kPa were considered, the average absolute value of the relative differences between model and measurements was lower than 3% for both tested fluids. All relative differences were within ±7%, with the only exception of a single point which had a 10% deviation.

For pressure drops lower than 1 kPa, the relative differences were slightly higher. In general, the lower pressure drop measured, the higher deviation was found: the highest deviation (15%) was found for a pressure drop of 0.2 kPa. Nevertheless, as the absolute difference between model and measurement in this case was equal to 0.04 kPa, this was well within the accuracy of the differential pressure sensor (0.1 kPa). Beside the accuracy of the instruments, other sources of error might be the assumptions made by the model, such as linear interpolation between laminar and turbulent conditions in case of transitional regime and fully developed flow throughout the pipes.

As expected, given the same temperature and flow rate, the pressure drop for the glycol/water mixture was larger than that of water, due to the much higher viscosity.

Additionally, the pressure drop for both fluids was higher at lower temperatures, due to the increased viscosity. Nevertheless, this effect was much more relevant for the 50% glycol/water mixture than for water. This was due to two main factors. Firstly, the kinematic viscosity of water decreases by a factor of 2.7 when the temperatures increases from 20 °C to 80 °C, while that of a 50% glycol/water mixture decreases by a factor of 5 for the same temperature variation. Secondly and more importantly, the higher viscosity characterizing the glycol/water mixture caused the Reynolds number in the horizontal pipes to be lower than 2300, meaning laminar flow regime. Even at the highest tested flow rate of 2.5 m^3 h^{-1}, the glycol/water mixture at 25 °C was still characterized by a completely laminar regime (Re<1500), entailing much higher friction factors compared to those at the higher temperatures.

Despite its secondary importance, also the higher density contributed in increasing the pressure drop at lower temperatures, and again the effect was more important for the glycol/water mixture, as its density varies by 3.8% in the range 20 °C-75 °C, compared to 2.3% for water.

Concerning the flow distribution, the results given by the model showed a decrease in flow rate from the top to the bottom pipes. This was the obvious consequence of the fact that only friction was considered as driving force for the flow distribution, so that the longer the hydraulic path, the higher the resistance.

A large difference appeared to exist when comparing flow distributions obtained for different flow regimes. Because of the weak dependence of the friction factor on the Reynolds number in the turbulent regime, the friction factor can been considered approximately constant in all horizontal pipes. Due to the geometry of the collector, the flow regime in most part of the manifold was turbulent, when it was turbulent in the horizontal pipes. This entailed that the pressure losses both in manifold segments and tees were relatively small compared to that occurring across the horizontal pipes, and it could be compensated by a slight unbalance in the collector flow distribution. As the pressure drop coefficients for tees in laminar regime are much higher than in turbulent regime and the laminar friction factor behaves similarly, the flow rate in the last tubes needed to diminish abruptly in order to cause the same pressure drop as the previous hydraulic paths.

When using water at 20 °C, the higher viscosity caused the flow regime inside the horizontal pipes to change from completely laminar to completely turbulent, depending on the flow rate (Figure 5). At 0.5 m^3 h^{-1}, the flow regime in all the horizontal pipes was laminar, while that in the manifold was initially turbulent and then, as more fluid was diverted to the horizontal pipes, laminar. The precise tee junction after which the change in flow regime occurred can be identified looking at the change in slope in the curves in Figure 5: a milder slope corresponds to turbulent flow in the manifold, while a steeper slope to laminar flow. The main reason for this behavior was that the local loss coefficients for tees in laminar regime are more sensitive to flow conditions than in turbulent regime, so they varied more significantly from one pipe to the next. As the hydraulic resistance between two consecutive pipes differed more significantly, this needed to be compensated by a larger difference in flow rates. A secondary reason is the linear dependence of the friction pressure drop on the flow rate in laminar conditions, which, compared to the quadratic dependence in turbulent conditions, required a larger variation in flow rate to compensate the varying pressure drop across the horizontal pipes.

Increasing the flow rate, the distribution became more uniform, as a longer part of the manifolds experienced turbulent conditions and the regime inside the horizontal pipes became transitional (V=1 m^3 h^{-1}) and then turbulent (V≥1.5 m^3 h^{-1}).

When using the presented model to evaluate the flow distribution in a solar collector, a user should keep in mind the assumptions and simplifications which were introduced, such as linear interpolation between laminar and turbulent friction factor for the transition region, fully developed flow along the horizontal pipes and manifold segments, and reliability of literature correlations when applied to the treated cases. The model was validated only in terms of overall pressure drop across the collector, and not in terms of flow distribution.

5. Conclusions

A model for estimating the pressure drop across a solar collector with U-type configuration in isothermal conditions was developed in Matlab. The model was validated against pressure drop measurements carried out on a HT-SA 35/10 collector in different conditions of flow rate, fluid type and temperature.

For pressure drops higher than 1 kPa, all relative differences between model and measurements were within ±7%, apart from one point. On average, the relative difference between model and measurements was within ±3%. For lower pressure drops the relative difference increased up to a maximum value of 15%, but always within the accuracy of the differential pressure sensor (0.1 kPa).

As expected, flow rate and viscosity were the main factors influencing the pressure drop, so different fluids having similar values for these two parameters gave almost identical pressure drops. This suggests a pressure drop curve for a glycol/water mixture at relatively high temperature can be evaluated using water at sufficiently low temperature, provided that in these conditions the two fluids have similar viscosity and density.

Regarding the flow distribution, it was found that this was mainly affected by the flow regime in the manifolds. Turbulent regime throughout the manifolds entailed a much more uniform flow distribution than laminar flow. This was mainly due to the strong dependence of the local losses for the tee junctions in laminar conditions, which caused relatively large difference in pressure drop even at small flow rate variation, as that occurring between two consecutive tees. If the presented model is used to evaluate the flow distribution in a solar collector, the introduced assumptions and simplifications must be taken carefully into account.

6. Acknowledgment

The first author is thankful to the Marie-Curie Actions - Initial Training Network research programme of the European Union which supported him through the SolNet-SHINE project. The authors are also grateful to the company Arcon-Sunmark A/S for having made available the HT-SA collector used during the study.

7. References

Binder, R.C., 1973. Fluid Mechanics, fifth ed. Prentice Hall.

Chiou, J.P., 1982. The effect of non-uniform fluid flow distribution on the thermal performance of solar collector. Solar Energy 29(6), 487-502.

Colebrook, C.F., 1939. Turbulent flow in pipes, with particular reference to the transition region between smooth and rough pipe laws. Journal of the Institution of Civil Engineers 11, 133-156.

ISO Standard 9806, 2014. Solar energy – Solar thermal collectors – Test methods.

Fan, J., Shah, L.J., Furbo, S., 2007. Flow distribution in a solar collector panel with horizontally inclined absorber strips. Solar Energy 81(12), 1501-1511.

Furbo, S., 2015. Using water for heat storage in thermal energy storage (tes) systems, in: Cabeza, L.C. (Ed.), Advances in Thermal Energy Storage Systems. Woodhead Publishing Series in Energy, pp. 31-47.

Haaland, S.E., 1983. Simple and Explicit Formulas for the Friction Factor in Turbulent Flow. Journal of Fluids Engineering (ASME) 105(1): 89-90.

Holman, J.P., 2002. Heat transfer, ninth ed. McGraw-Hill, New York.

Idelchik, I.E., 1994. Handbook of hydraulic resistance, third ed. CRC press.

Jones, G.F., Lior, N., 1994. Flow distribution in manifolded solar collectors with negligible buoyancy effects. Solar Energy 52(3), 289-300.

Joseph, D.D., Yang B.H., 2010. Friction factor correlations for laminar, transition and turbulent flow in smooth pipes. Physica D 239, 1318-1328.

Kestin, J., Sokolov, M., Wakeham, W.A., 1978. Viscosity of liquid water in the range -8 °C to 150 °C. Journal of Physical and Chemical Reference Data 7, 941-948.

Kovacs, P., Persson, M., Wahlgren, P., Jensen, S., 2012. Quality assurance in solar thermal heating and cooling technology - Pressure drop over a solar flat plate collector using various heat transfer fluids. Deliverable D2.2 – R2.13 of Project IEE/08/593/SI2.529236 supported by Intelligent Energy Europe. [Available online at http://www.estif.org/, accessed on 18/09/2015]

Ohnewein, P., Hausner, R., Preiß, D., 2015. Hydraulikdesign von parallelen Kollektormodulen in solarthermischen Großanlagen. Neue Energien 2020 – ParaSol project (preliminary version, from personal comunication with Ohnewein P.).

Wang, X.A., Wu, L.G., 1990. Analysis and performance of flat plate solar collector arrays. Solar Energy 45(2), 71-78.

Weitbrecht, V., Lehmann, D., Richter, A., 2002. Flow distribution in solar collectors with laminar flow conditions. Solar Energy 73(6), 433-441.

Windeleff, J., Nielsen, J.E., 2014. Solar District Heating in Denmark. Danish Energy Agency and PlanEnergi.